Structure and Solution Dynamics of $[(Ph_3P)_2Pd(Ph)(FHF)]$†

D. Christopher Roe,* William J. Marshall, Fredric Davidson, Paul D. Soper, and Vladimir V. Grushin*

Central Research and Development, E. I. du Pont de Nemours and Co. Inc., Experimental Station, Wilmington, Delaware 19880-0328

Received July 24, 2000

The bifluoride complex *trans*-$[(Ph_3P)_2Pd(Ph)(FHF)]$ (**1**) was studied by single-crystal X-ray diffraction, IR, and variable-temperature ^1H, ^{19}F, and ^{31}P NMR spectroscopy. Like other transition-metal bifluorides, **1** exhibits fluxional behavior (NMR) in solution at room temperature. When exchange processes are frozen (−60 °C), the solution structure of **1** is consistent with the solid-state X-ray data. Although all structural and spectroscopic data point to MF···HF rather than M···FHF character for **1**, ^{19}F NMR magnetization transfer experiments demonstrated a minor contribution of HF dissociation to the exchange. The main process that governs F/F exchange in **1** is intramolecular ($\Delta H^{\ddagger} = 33.7 \pm 2.1$ kJ mol^{-1}; $\Delta S^{\ddagger} = -56.1 \pm 9.6$ J mol^{-1} K^{-1}), likely occurring via pentacoordinate $[(Ph_3P)_2Pd(Ph)(\eta^2$-FHF)], in which both fluorines are coordinated to Pd. DFT calculations for two model Pd bifluoride complexes $[(R_3P)_2Pd(Me)(FHF)]$ (R = H, Me) indicated virtually unrestricted rotation around the Pd−FHF bond.

Introduction

In recent years, considerable progress has been made in the new, rapidly growing field of late-transition-metal fluorides.[1] The remarkable ability of transition-metal fluorides to promote/catalyze various organic reactions[1−4] can be influenced dramatically via interactions of the M−F bond with small molecules, especially hydrogen bond donors.[5,6] Of special significance are rarely reported[5] H-interactions of metal fluorides with the most commonly occurring H_2O and HF which often forms upon hydrolysis of the M−F bond. Valuable information on the nature of hydrogen bonding between M−F species and HF may be therefore obtained by studying transition-metal bifluorides, $[L_nM-FHF]$.

Transition-metal bifluoride complexes are rare. Since the report of $[(Et_3P)_2Pt(Ph)(FHF)]$ by Coulson[7] 25 years ago, only eight transition-metal species containing a terminal FHF ligand have been described in the literature.[7−14] Of those, only six have been isolated in pure form[7,9−11] and only four have been structurally characterized.[9,10,13] Even less information has been accrued on solution behavior of the M−FHF species, all of which appear to be fluxional.[7−13] Both HF dissociation (eq 1)[8,10] and M−FHF ionization (eq 2)[9,12] have been tentatively proposed to govern the exchange processes. However, no detailed studies elucidating mechanisms of solution dynamics for a transition-metal bifluoride have been reported to date.

$$[L_nM\text{-}F\text{-}H\text{-}F] \rightleftharpoons [L_nM\text{-}F] + H\text{-}F \qquad (1)$$

$$[L_nM\text{-}F\text{-}H\text{-}F] \rightleftharpoons [L_nM]^+ + F\text{-}H\text{-}F^- \qquad (2)$$

In this paper, we report an X-ray structure and solution behavior of a palladium bifluoride complex, *trans*-$[(Ph_3P)_2Pd(Ph)(FHF)]$ (**1**).[11] Remarkably, neither HF dissociation nor Pd−F ionization (eqs 1 and 2) appears to govern the fast exchange process that occurs in solutions of **1**. Complex **1** is the first transition-metal

† Contribution No. 8027.

(1) For reviews of transition metal fluoro complexes and C−F activation, see: (a) Doherty, N. M.; Hoffmann, N. W. *Chem. Rev.* **1991**, *91*, 553. (b) Kiplinger, J. L.; Richmond, T. G.; Osterberg, C. E. *Chem. Rev.* **1994**, *94*, 373. (c) Murphy, E. F.; Murugavel, R.; Roesky, H. W. *Chem. Rev.* **1997**, *97*, 3425. (d) Plenio, H. *Chem. Rev.* **1997**, *97*, 3363. (e) Richmond, T. G. *Top. Organomet. Chem.* **1999**, *3*, 243.

(2) Grushin, V. V. *Angew. Chem., Int. Ed. Engl.* **1998**, *37*, 994.

(3) Dorta, R.; Egli, P.; Zuercher, F.; Togni, A. *J. Am. Chem. Soc.* **1997**, *119*, 10857. Krueger, J.; Carreira, E. M. *J. Am. Chem. Soc.* **1998**, *120*, 837. Pagenkopf, B. L.; Carreira, E. M. *Tetrahedron Lett.* **1998**, *39*, 9593; *Chem. Eur. J.* **1999**, *5*, 3437.

(4) (a) Bennett, B. K.; Harrison, R. G.; Richmond, T. G. *J. Am. Chem. Soc.* **1994**, *116*, 11165. (b) Barthazy, P.; Hintermann, L.; Stoop, R. M.; Worle, M.; Mezzetti, A.; Togni, A. *Helv. Chim. Acta* **1999**, *82*, 2448.

(5) For a review, see: Richmond, T. G. *Coord. Chem. Rev.* **1990**, *105*, 221.

(6) Patel, B. P.; Crabtree, R. H. *J. Am. Chem. Soc.* **1996**, *118*, 13105. Lee, D.-H.; Kwon, H. J.; Patel, B. P.; Liable-Sands, L. M.; Rheingold, A. L.; Crabtree, R. H. *Organometallics* **1999**, *18*, 1615. Brammer, L.; Bruton, E. A.; Sherwood, P. *New J. Chem.* **1999**, *23*, 965.

(7) Coulson, D. R. *J. Am. Chem. Soc.* **1976**, *98*, 3111.

(8) Hintermann, S.; Pregosin, P. S.; Rüegger, H.; Clark, H. C. *J. Organomet. Chem.* **1992**, *435*, 225.

(9) (a) Whittlesey, M. K.; Perutz, R. N.; Greener, B.; Moore, M. H. *J. Chem. Soc., Chem. Commun.* **1997**, 187. (b) Whittlesey, M. K.; Perutz, R. N.; Moore, M. H. *J. Chem. Soc., Chem. Commun.* **1996**, 787.

(10) (a) Murphy, V. J.; Hascall, T.; Chen, J. Y.; Parkin, G. *J. Am. Chem. Soc.* **1996**, *118*, 7428. (b) Murphy, V. J.; Rabinovich, D.; Hascall, T.; Klooster, W. T.; Koetzle, T. F.; Parkin, G. *J. Am. Chem. Soc.* **1998**, *120*, 4372.

(11) (a) Fraser, S. L.; Antipin, M. Yu.; Khroustalyov, V. N.; Grushin, V. V. *J. Am. Chem. Soc.* **1997**, *119*, 4769. (b) Pilon, M. C.; Grushin, V. V. *Organometallics* **1998**, *17*, 1774.

(12) Gil-Rubio, J.; Weberndöfer, B.; Werner, H. *J. Chem. Soc., Dalton Trans.* **1999**, 1437.

(13) Braun, T.; Foxon, S. P.; Perutz, R. N.; Walton, P. H. *Angew. Chem., Int. Ed.* **1999**, *38*, 3326. See also Archibald, S. J.; Braun, T.; Gaunt, J. A.; Hobson, J. E.; Perutz, R. N. *J. Chem. Soc., Dalton Trans.* **2000**, 2013.

(14) A dinuclear niobium complex containing two μ-FHF ligands has been structurally characterized: Roesky, H. W.; Sotoodeh, M.; Xu, Y. M.; Schrumpf, F.; Noltemeyer, M. Z. *Anorg. Allg. Chem.* **1990**, *580*, 131.

10.1021/om000637r CCC: $19.00
Publication on Web 09/20/2000

Table 1. Selected Crystallographic Data for *trans*-[$(Ph_3P)_2Pd(Ph)(FHF)$] (1)

empirical formula	$C_{42}H_{36}F_2P_2Pd$
fw	747.05
cryst size, mm	0.23 × 0.24 × 0.40
cryst syst	monoclinic
space group	$P2_1$ (No. 4)
temp, K	173
a, Å	12.062(1)
b, Å	26.719(1)
c, Å	12.455(1)
β, deg	118.76(1)
V, Å^3	3518.7(4)
Z	4
calcd density, g cm^{-3}	1.410
μ(Mo), mm^{-1}	0.66
diffractometer	Bruker SMART 1K CCD
2θ range, deg	3.04−61.04
scan type	ω
correction	SADABS
no. of rflns collected	69 051
no. of unique rflns used in refinement ($I > 4.0\sigma(I)$)	20 496
data to param ratio	23.97
R1, %	3.28
wR2, %	6.72
goodness of fit	1.07

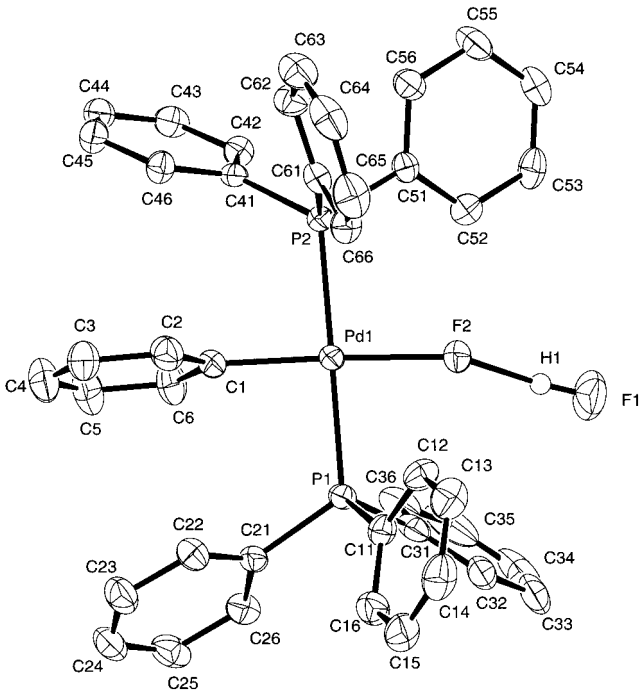

Figure 1. Molecular structure of [$(Ph_3P)_2Pd(Ph)(FHF)$] (**1**; one of the two independent molecules). For selected bond distances and bond angles, see Table 2.

bifluoride for which both a solid-state structure and mechanisms of exchange in solution have been established.

Results

Single-Crystal X-ray Structure of *trans*-[$(Ph_3P)_2Pd(Ph)(FHF)$] (1). X-ray-quality crystals of **1** were obtained from dichloromethane−hexane. Selected crystallographic data for **1** are collected in Table 1. Figure 1 presents an ORTEP drawing of one of the two structurally similar molecules in the asymmetric unit.

Structural data have been used to assess π-effects of the F ligand in palladium fluoride complexes.[15,16] It has been shown[15] that for a series of square-planar [$(Ph_3P)_2$-Pd(Ph)(X)], where X = F (**2**), Cl (**3**), Br (**4**), I (**5**), certain geometry parameters depend on the π-donating ability of the halogen X. The following parameters are particularly important.

(1) For X = Br and I, weak π-donors, the angle between the coordination plane of the complex and the σ-phenyl ring is close to 90°, whereas for the strongly π-donating Cl and F this angle deviates considerably from the ideal value. This way a compromise is found between Pd−X bond destabilization due to $d_\pi-p_\pi$ filled/filled repulsions[17] and perturbation of the aromatic system via push−pull interactions between p_π on X and aromatic π^* through filled d orbitals on Pd.[15]

(2) The ipso angle C−C−C at the Pd−substituted phenyl carbon increases in the series X = F < Cl < Br < I, indicating a decrease in the electron-donating properties of the $Pd(Ph_3P)_2X$ group on going from the lighter to heavier halide ligands. This so-called "halogen anomaly" is due to a decrease in the π-donating strength of the halides in the order F > Cl > Br > I.[15,17]

(3) The conformation along the P−Pd−P axis is remarkably distinct for X = F, Cl (eclipsed) and X = Br, I (twisted).[15] The eclipsed conformation favors Pd−F···H−C(phosphine) interactions,[16] which alleviate the filled/filled repulsions. Such interactions have also been observed for tertiary phosphine fluoro complexes of other metals.[1,4b]

Table 2 summarizes important geometry parameters for **1**−**5**. Analysis of these parameters within the Pd(Ph)(X)$(P)_2$ coordination core indicates that the molecular structure of **1** (X = FHF) is distinct from those of **2** and **3** (X = F and Cl, strongly π-donating halogens) but remarkably similar to **4** and **5** containing heavier Br and I, much weaker π-donors. In particular, like the bromo (**4**) and iodo (**5**) complexes, bifluoride **1** exhibits a twisted orientation of the phosphines along the P−Pd−P axis, whereas a distinct eclipsed conformation is observed for the fluoride **2** and chloride **3**. In accord with this observation, no short Pd−F···H−C(phosphine) contacts are found in the X-ray structure of **1**. The dihedral angle formed by the mean coordination plane and the π-phenyl ring in **1** (81.1 and 81.3°) is larger than in **2** (71.5°) and **3** (75.4°), while approaching the values determined for **4** (86.0°) and **5** (84.2°). The averaged Pd−P bond distance in **1** is longer than in **2** but shorter than in **5**. The C−C−C bond angle at the ipso carbon of the π-phenyl ligand in **1** (118.5(2) and 118.3(2)°) is between the values measured for **2** (117.0(5)°) and **5** (119.2(4)°). Therefore, the structural evolution observed on going from **2** and **3** to **4**, **5**, and **1** points to a decrease in the π-donating ability of the F ligand in **2** upon HF coordination, as expected. Consequently, the push−pull interactions along the Ar−Pd−X axis decrease in the order X = F > FHF ≈ Br ≈ I.

The Pd−F bond in **1** (2.098(2) and 2.103(2) Å) is elongated as compared with **2** (Pd−F = 2.085(3) Å),[11a] whereas the Pd−C bond distances in **1** (1.989(2) and 1.994(2) Å) and in **2** (1.998(5) Å) are only marginally different. The F···F separation (ca. 2.35 and 2.36 Å) found in **1** is significantly longer than in [$(dmpe)_2$Ru-

(15) Flemming, J. P.; Pilon, M. C.; Borbulevitch, O. Ya.; Antipin, M. Yu.; Grushin, V. V. *Inorg. Chim. Acta* **1998**, *280*, 87.
(16) Marshall, W. J.; Thorn, D. L.; Grushin, V. V. *Organometallics* **1998**, *17*, 5427.
(17) Caulton, K. G. *New J. Chem.* **1994**, *18*, 25.

Table 2. Selected Geometry Parameters for the Complexes *trans*-[(Ph$_3$P)$_2$Pd(Ph)(X)] (X = FHF (1), F (2), Cl (3), Br (4), I (5))

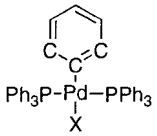

param	**1** (X = FHF)	**2** (X = F)[11a]	**3** (X = Cl)[15]	**4** (X = Br)[15]	**5** (X = I)[15]
			Interatomic Distances, Å		
Pd-X	2.098(2); 2.103(2)	2.085(3)	2.407(1)	2.532(1)	2.701(1)
Pd−C	1.989(2); 1.994(2)	1.998(5)	2.016(3)	1.995(6)	2.029(4)
Pd−P	2.3242(7); 2.3084(7)	2.315(1)	2.316(1)	2.322(2)	2.338(1)
Pd−P	2.3313(7); 2.3275(7)	2.318(1)	2.324(1)	2.327(2)	2.342(1)
			Bond Angles, deg		
C−Pd−X	175.5(1); 176.6(1)	179.0(2)	179.8(1)	171.5(2)	171.4(1)
P−Pd−P	178.50(3); 177.62(3)	174.24(5)	177.55(2)	175.04(5)	173.81(4)
P−Pd−X	85.71(5); 87.01(5)	86.57(9)	88.57(2)	89.94(5)	90.87(3)
P−Pd−X	94.47(5); 94.47(5)	89.90(9)	89.75(2)	95.01(4)	95.24(3)
P−Pd−C	88.14(7); 86.67(7)	91.1(1)	90.29(7)	86.3(2)	86.1(1)
P−Pd−C	91.59(7); 91.75(7)	92.5(1)	91.38(7)	88.9(2)	88.0(1)
C−C−C	118.5(2); 118.3(2)	117.0(5)	117.8(3)	117.9(6)	119.2(4)
			Interplanar Angle, σ-Ph/Pd coordination plane, deg		
	81.1; 81.3	71.5	75.4	86.0	84.2
			Phosphine Conformation along the P−Pd−P Axis		
	twisted	eclipsed	eclipsed	twisted	twisted

(H)(FHF)] (ca. 2.28 Å)[9] and more comparable to the values determined for [(Me$_3$P)$_4$MH$_2$F(FHF)] (M = Mo, W; 2.35−2.39 Å)[10] and for [(Et$_3$P)$_2$Ni(C$_3$N$_2$F$_2$)(FHF)] (2.40 Å).[13] All structural parameters and the IR data for **1** (ν_{HF} 2578 and 1822 cm^{-1} in KBr) indicate that although the hydrogen-bonding interaction within the PdFHF unit is strong, **1** is more similar to [Pd−F···H−F] than to the [Pd···F−H−F] extreme. The large Pd−F···F angles of 153.6 and 153.4° found in **1** are likely due to residual push−pull interactions along the Ph−Pd−F axis. Indeed, a large Ni−F···F angle of 156.7° has been found in [(Et$_3$P)$_2$Ni(C$_3$N$_2$F$_2$)(FHF)],[13] for which push−pull interactions with the trans σ-difluoropyrimidyl ligand are as conceivable. In contrast, the M−F··· F angle is noticeably smaller (130−134°) in the structures of the Ru,[9] Mo, and W[10] bifluorides and also *trans*-[(Ph$_3$P)$_2$Pd(Me)(FHF)],[18] which are all devoid of such interactions.

NMR Characterization of 1. All NMR experiments were carried out using freshly prepared solutions of **1** in rigorously dry CD_2Cl_2 and toluene-d_8 (2/1 v/v). The solutions were placed in Teflon liners inside standard 5 or 10 mm glass NMR tubes that were sealed with rubber septa. At room temperature, a broad singlet at 12.5 ppm was present in the ^{1}H NMR spectrum of **1**, a slightly broadened singlet at 22.9 ppm was observed in the ^{31}P NMR spectrum, and all ^{19}F NMR signals were too broad to be detected. At −60 °C, the proton resonance at 12.5 ppm was resolved into a doublet of doublets with J_{F-H} = 368 and 33 Hz, and the ^{31}P{^{1}H} NMR signal appeared as a doublet (J_{P-F} = 8 Hz). Two multiplet resonances of equal intensity were observed in the ^{19}F NMR spectrum at −60 °C, a doublet of doublets at −174 ppm (J_{H-F} = 368 Hz; J_{F-F} = 119 Hz) due to the terminal fluorine, PdFH*F*, and a doublet of doublet of triplets at −254 ppm (J_{H-F} = 33 Hz; J_{F-F} = 119 Hz; J_{F-P} = 8 Hz) from Pd*F*HF.[19] The latter resonance transformed into a doublet of doublets (J_{H-F} = 33 Hz; J_{F-F} = 119 Hz) when the spectrum was rerun with ^{31}P decoupling (Figure 2). In accord with this observation, the doublet ^{31}P NMR signal was observed as a singlet in the ^{31}P NMR spectrum with ^{1}H and ^{19}F decoupling (Figure 3). Hence, the structure of **1** in solution at −60 °C (Figure 4) was fully consistent with the solid-state X-ray data (Figure 1).

Dynamic NMR Studies of 1. The variable-temperature (VT) NMR studies (see above) clearly indicated that in solution **1** undergoes exchange that is fast on the NMR time scale at room temperature but can be frozen out at −60 °C. To shed light on the mechanism of this exchange, solutions of **1** were studied by ^{19}F NMR magnetization transfer.

NMR spectroscopy is a versatile tool for the study of chemical kinetics by virtue of the wide range of rates that may be measured.[20,21] When the exchange rate

(18) (a) Although in the structure of *trans*-[(Ph$_3$P)$_2$Pd(Me)(FHF)][18b] the methyl group and FHF were disordered across the center of symmetry (Pd), the F···F separation (2.31 Å) and the Pd−F···F bond angle (132.8°) could be determined. These values and the IR data for [(Ph$_3$P)$_2$Pd(Me)(FHF)] (ν_{HF} 2493 and 1904 cm^{-1}) indicate that hydrogen bonding is stronger in the methyl complex than in **1**, possibly due to the lack of push−pull interactions with the electron-donating methyl group. (b) Marshall, W. J.; Grushin, V. V. Unpublished results, 1998.

(19) (a) At −60 °C, both PdF*H*F and Pd*F*HF NMR signals were broadened, much like the corresponding resonances from [(dmpe)$_2$Ru(H)(FHF)].[9] It is unclear if short relaxation times or some other factors were responsible for the line width observed. Running the NMR spectra of **1** below −60 °C did not result in line shape improvement but rather distortion and lower resolution, possibly due to viscosity increase and/or restricted rotation around the Pd−P and Pd−Ph bonds.[19b,c] (b) In the strongly hydrogen bonded system A···H···B the proton motion can have a vanishingly small barrier and hence cannot be frozen out even at very low temperatures. See: Golubev, N. S.; Shenderovich, I. G.; Smirnov, S. N.; Denisov, G. S.; Limbach, H.-H. *Chem. Eur. J.* **1999**, *5*, 492. (c) For examples of restricted rotation around M−Ar bonds (M = Pt, Pd), see: Brown, J. M.; Pérez-Torrente, J. J.; Alcock, N. W. *Organometallics* **1995**, *14*, 1195. Brown, J. M.; Pérez-Torrente, J. J.; Alcock, N. W.; Clase, H. J. *Organometallics* **1995**, *14*, 207. Vicente, J.; Abad, J.-A.; Fernández-de-Bobadilla, R.; Jones, P. G.; Ramírez de Arellano, M. C. *Organometallics* **1996**, *15*, 24. Vicente, J.; Abad, J.-A.; Rink, B.; Hernández, F.-S.; Ramírez de Arellano, M. C. *Organometallics* **1997**, *16*, 5269.

(20) Jackman, L. M., Cotton, F. A., Eds. *Dynamic Nuclear Magnetic Resonance Spectrsocopy*; Academic Press: New York, 1975.

(21) Sandström, J. *Dynamic NMR Spectroscopy*; Academic Press: New York, 1982.

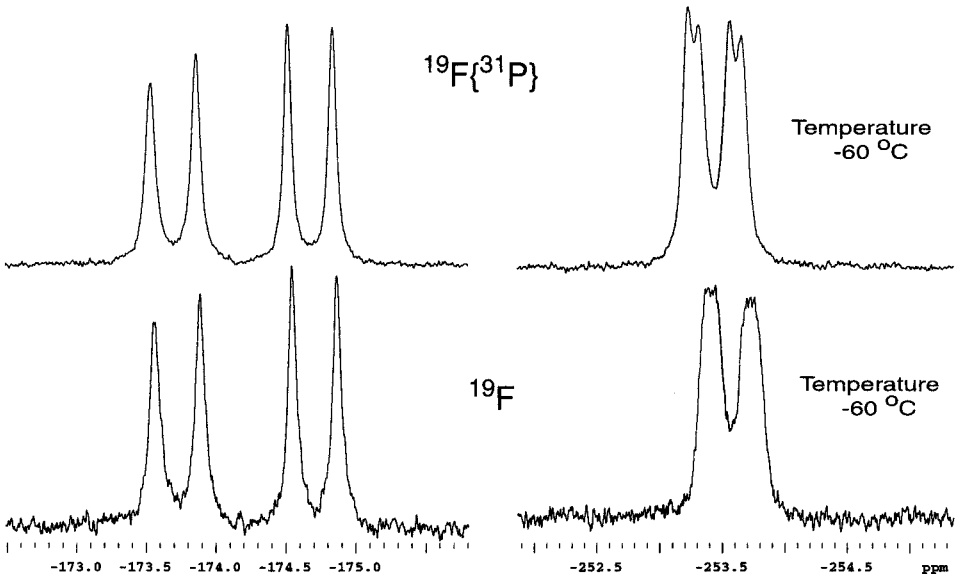

Figure 2. $^{19}F\{^{31}P\}$ (top) and ^{19}F (bottom) NMR spectra of **1** at −60 °C.

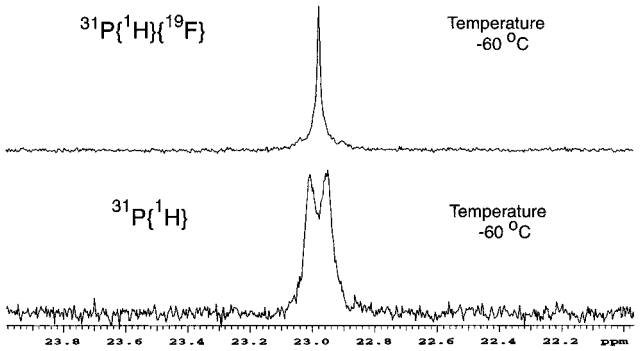

Figure 3. $^{31}P\{^{1}H,^{19}F\}$ (top) and $^{31}P\{^{1}H\}$ (bottom) NMR spectra of **1** at −60 °C.

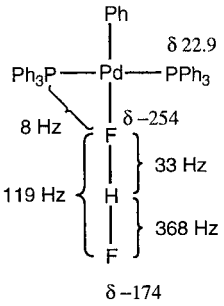

Figure 4. Spin−spin coupling constants for **1**, as determined by VT NMR experiments.

between distinct chemical shift sites is comparable to the spin relaxation rates $1/T_1$, magnetization transfer may be used as a technique to derive rate constants and activation parameters for the exchange process.[21] T_1 is the exponential time constant for magnetization to return to its Boltzmann equilibrium following a perturbation, and when an exchange site is *selectively* perturbed either by saturation[22] or by a 180° pulse,[23,24] its apparent T_1 is decreased and the resonances of the exchange partners undergo a transient decrease in intensity on the time scale of the T_1 recovery.

Like the VT NMR studies above, the magnetization transfer experiments were conducted in a 2/1 (by volume) mixture of rigorously dry CD_2Cl_2 and toluene-d_8, in Teflon liners placed inside standard 5 or 10 mm glass NMR tubes sealed with rubber septa.

The first series of the magnetization transfer experiments were carried out with [**1**] = 1.6×10^{-2} M. As we kept in mind the possibility of HF and/or FHF^- dissociation (eqs 1 and 2), the measurements were repeated with a considerably lower concentration, [**1**] = 1.9×10^{-3} M, to slow the exchange and possibly determine its order. This 8-fold dilution, however, did not result in an observable rate change, as judged by dynamic line shape changes from −20 to −80 °C, suggesting an *intramolecular* mechanism for the exchange.

To investigate the possibility of HF dissociation from **1**, the exchange was studied with samples containing both **1** and its fluoride analogue $[(Ph_3P)_2Pd(F)(Ph)]$ (**2**), in different ratios; i.e., sample **A**, **1**/**2** = 95/5 ([**1**] = 1.9×10^{-3} M; [**2**] = 0.1×10^{-3} M); sample **B**, **1**/**2** = 50/50 ([**1**] = 2.3×10^{-3} M; [**2**] = 2.3×10^{-3} M). In the case of intramolecular exchange between internal and terminal fluorines in Pd−FHF in the presence of Pd−F, we were able to follow the intensities of the well-resolved resonances (Pd−FH*F* at δ −174 ppm, Pd−*F*HF at δ −254 ppm, and Pd−*F* at δ −275 ppm[11]) from −80 °C either to −40 °C for sample **A** or to −30 °C for sample **B**. A slower *intermolecular* exchange process between the metal-bound fluoride Pd−*F*HF and the fluoride of **2** (see below) could be followed from −70 to −30 °C. Below the lower temperature limit, the intensity changes were too small to be reliably quantitated, while above the indicated upper temperature limits, line broadening indicative of fast exchange precluded continued application of this "slow exchange" method.

The experimental procedure for studying the exchange processes at a given temperature involves selectively inverting the Pd−*F*HF resonance and monitoring the intensities at the Pd−FH*F* and Pd−*F* sites in addition to the recovery of intensity at the Pd−*F*HF site. This procedure is then repeated by inverting the Pd−FH*F* resonance and then inverting the Pd−*F* site. The three data sets for the given temperature are

(22) Forsen, S.; Hoffman, R. A. *J. Chem. Phys.* **1963**, *39*, 2892; **1964**, *40*, 1189.
(23) Alger, J. R.; Prestegard, J. H. *J. Magn. Reson.* **1977**, *27*, 137.
(24) Roe, D. C. *Organometallics* **1987**, *6*, 942.

combined and analyzed jointly to give the best fitting rate constants. Since the details of the exchange process are not known with certainty, the apparent exchange mechanism can be evaluated by consideration of the exchange matrix which describes the process. To facilitate a description of the exchange process in terms of an exchange matrix, Pd−FH*F* is labeled as site 1, Pd−*F*HF as site 2, and Pd−*F* as site 3. If it is presumed, for the moment, that exchange between Pd−*F*HF and Pd−FH*F* is intramolecular (see above), the exchange rate constant between sites 1 and 2 may be labeled k_1 without regard for the specific concentration of **1**. On the other hand, exchange between Pd−FHF and Pd−F is clearly intermolecular, and if the exchange of Pd−*F* involves Pd−*F*HF (HF transfer), then the exchange rate for site 3 may be labeled k_2 while for site 2 this process contributes k_2[3]/[2] (in order to maintain mass balance). The net result of this exchange matrix description is a model which allows for intramolecular exchange between Pd−*F*HF and Pd−FH*F*, intermolecular exchange between Pd−*F*HF and Pd−*F*, and no direct exchange process involving Pd−FH*F* and Pd−*F*.

A qualitative description of the exchange process is available by examination of the magnetization transfer results for sample **B**, for example at −50 °C (see Figure 5A). Selective inversion of Pd−FH*F* (circles) results in moderately fast magnetization transfer to Pd−*F*HF (squares) and barely perceptible transfer to Pd−*F* (diamonds). Figure 5B involves selective inversion of Pd−*F*HF, which again leads to evident magnetization transfer to Pd−FH*F* and noticeable transfer to Pd−*F*, while Figure 5C shows that selective inversion of Pd−*F* leads to approximately equal perturbation at both Pd−FH*F* and Pd−*F*HF. The immediate interpretation of these results involves rapid exchange between Pd−*F*HF and Pd−FH*F* and rather slower exchange between Pd−*F*HF and Pd−*F* consistent with the model presented in the previous paragraph.

The validity of the presented model can be tested quantitatively by allowing for the possibility of direct exchange between Pd−FH*F* and Pd−*F* by letting the exchange rate for site 3 be k_3, with the consequence that this process contributes to the exchange at site 1 by an amount k_3[3]/[1] (i.e., in addition to k_1). This approach amounts to a model-free analysis of the exchange processes, since the number of independent rate constants for three sites is 3 ($n(n-1)/2$ for n sites). The appropriate exchange matrix is

$$\begin{pmatrix} -k_1 - k_3[3]/[1] & k_1 & k_3 \\ k_1 & -k_1 - k_2[3]/[2] & k_2 \\ k_3[3]/[1] & k_2[3]/[2] & -k_2 - k_3 \end{pmatrix}$$

The greatest opportunity for determining the importance of k_3 occurs at −30 °C, where this slow but potentially mechanistically important pathway would have its largest effect. The resulting best-fitting rate constants with standard deviations at −30 °C are $k_1 = 335 \pm 14$, $k_2 = 34 \pm 3$, and $k_3 = 1 \pm 3$ s^{-1}. The mechanistic inference of the result for k_3 is that the postulated exchange involving Pd−FH*F* and Pd−*F* is immaterial for describing the overall exchange process, since the standard deviation associated with the parameter determination is significantly larger than the parameter itself. The remainder of the analysis was conducted with the exchange matrix below, which is appropriate for the first model presented (see above):

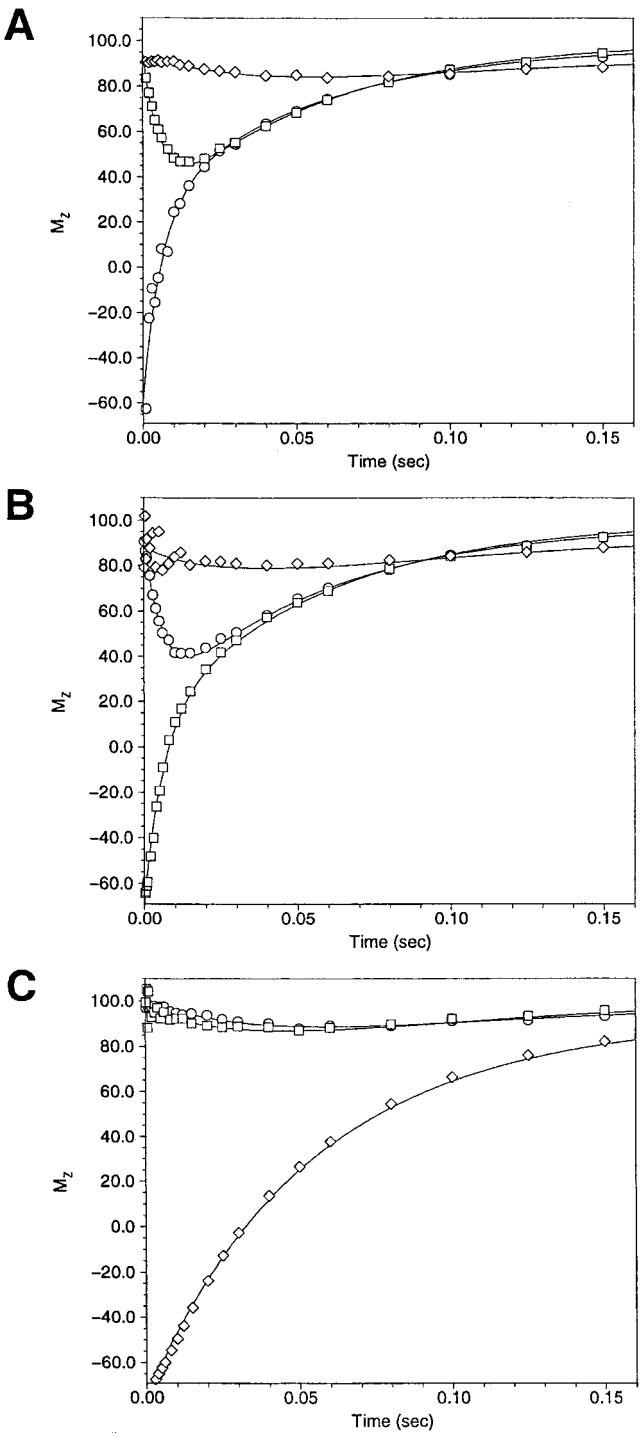

Figure 5. Magnetization transfer results at −50 °C for (A) selective inversion of Pd−FH*F* (○), (B) selective inversion of Pd−*F*HF (□), and (C) selective inversion of Pd−*F* (◇). Data were acquired out to 0.4 s. Solid lines are derived from least-squares fitting of the model involving three sites and two exchange processes (see text).

$$\begin{pmatrix} -k_1 & k_1 & 0 \\ k_1 & -k_1 - k_2[3]/[2] & k_2 \\ 0 & k_2[3]/[2] & -k_2 \end{pmatrix}$$

The details of the intramolecular rate analysis are presented in Table 3. It is clear that the intramolecular

Table 3. Magnetization Transfer Rate Constant k_1 for Intramolecular Fluorine Exchange in Pd−FHF as a Function of Temperature[a]

	k_1, s^{-1}		
T, °C	sample **A**	sample **B**	average
−80	3.7 (0.7)	3.0 (0.9)	3.4 (0.6)
−70	11.9 (0.8)	12.1 (0.9)	12.0 (0.6)
−60	31.9 (1.6)	27.4 (1.0)	28.7 (0.8)
−50	76.5 (2.4)	74.1 (2.4)	75.3 (1.7)
−40	179.3 (5.5)	176.6 (5.6)	178.0 (3.9)
−30	335.5 (14.3)	*b*	

[a] Standard deviation in parentheses. [b] Not determined.

Table 4. Magnetization Transfer Rate Constant k_2 for Intermolecular Exchange of Pd−FHF with Pd−F (sample B) as a Function of Temperature[a]

T, °C	k_2, s^{-1}	T, °C	k_2, s^{-1}
−70	1.46 (0.49)	−40	12.7 (0.54)
−60	3.34 (0.45)	−30	33.8 (0.91)
−50	6.71 (0.46)		

[a] Standard deviation in parentheses.

exchange rate constants k_1 are the same for sample **A** and sample **B** and that it is appropriate to use the weighted average of these results to describe the rate process. These results indicate that intermolecular exchange with Pd−F is not involved in the internal fluorine scrambling in Pd−FHF (consistent with the qualitative description given above). Activation parameters for this intramolecular exchange in Pd−FHF were determined by fitting the temperature dependence of the rate constants in Table 3 directly to the Eyring equation using a nonlinear least-squares program, while using the standard deviation as the estimated error in the rate constant and assuming ±2 °C as the estimated error in the actual temperature. The results of this analysis lead to estimates for the key activation parameters for this process of $\Delta H^{\ddagger} = 33.7 \pm 2.1$ kJ mol^{-1} and $\Delta S^{\ddagger} = -56.1 \pm 9.6$ J mol^{-1} K^{-1}, where the errors represent 95% confidence limits. At −50 °C, $\Delta G^{\ddagger} = 46.1 \pm 0.2$ kJ mol^{-1}.

The concentration of **2** in sample **A** was insufficient to permit quantitative magnetization transfer analysis. However, results for k_2 were obtained for sample **B** using the above three-site model, and rate constants from −30 to −70 °C are presented in Table 4. Activation parameters for intermolecular exchange between Pd−*F* and Pd−*F*HF are $\Delta H^{\ddagger} = 29.7 \pm 6.3$ kJ mol^{-1} and $\Delta S^{\ddagger} = -92.9 \pm 27.6$ J mol^{-1} K^{-1}, with $\Delta G^{\ddagger}(-50\ °C) = 50.5 \pm 0.4$ kJ mol^{-1}.

DFT Calculations. To gain further insight into the nature of the Pd−FHF bond of **1**, DFT calculations were performed for hypothetical *trans*-[$(PR_3)_2Pd(CH_3)FHF$] (R = H, Me) as model compounds, in which the phenyl ring bound to palladium was replaced by CH_3 and the two triphenylphosphine groups were replaced by PH_3 or PMe_3. Selected calculated geometry parameters are collected in Table 5. As opposed to the X-ray structures, the DFT calculations effectively treat the molecules as completely isolated. The differences in geometry are caused both by the differing ligands and by the greater freedom of movement of the HF fragment in the calculated structures.

Calculations were performed at a number of constrained F−F−Pd−P dihedral angles, while all other degrees of freedom were allowed to relax to their optimum values. There is essentially no energy barrier to rotation of that dihedral angle. Both the perpendicular and in-plane structures are only about 1 J mol^{-1} higher in energy than the optimum (6.8 and 46.4° for R = H and Me, respectively). The value of 1 J mol^{-1}, well below the accuracy of this level of theory, indicated virtually unrestricted rotation around the Pd−FHF bond. In accord with this, (i) no sign of restricted rotation around this bond was found during the VT NMR studies of **1** and (ii) the two otherwise similar independent molecules in the X-ray structure of **1** displayed remarkably different torsion angles F−F−Pd−P of 85.6 and 53.9°. The essentially flat potential energy surface caused our efforts to locate transition states for rotation or for FHF "slipping" across the coordination plane to be unsuccessful. The calculated enthalpies of reaction for addition of HF to the F ligand in the gas phase were the same for both model compounds at −87.9 kJ mol^{-1}.

Table 5. Selected Geometry Parameters Determined for 1 (X-ray) and Calculated for *trans*-[$(PR_3)_2Pd(CH_3)(FHF)$] (R = H, Me).

		DFT calculation on *trans*-[$(PR_3)_2Pd(CH_3)(FHF)$]	
param	X-ray data for **1**	R = H	R = Me
Pd−F (Å)	2.098; 2.103	2.176	2.152
(FH)−F (Å)	1.548; 1.615	1.364	1.379
F(H)−F−Pd (deg)	153.6; 153.4	98.5	105.9
F−F−Pd−P (deg)	85.6; 53.9	6.8	46.4

Discussion

Two types of transition-metal bifluoride complexes have been identified, i.e., M−F···H−F (e.g., [$(Me_3P)_4MH_2F(FHF)$], where M = Mo, W),[10] and M···F−H−F ([$(dmpe)_2Ru(H)(FHF)$]).[9] The X-ray, IR, and VT NMR data above indicate that **1** and its σ-methyl analogue are both of Pd−F···H−F rather than Pd···F−H−F character. Although the F−H distances in **1** cannot be measured accurately by X-ray diffraction, both the IR and NMR data above point to strongly asymmetric hydrogen-bonding interactions within the FHF ligand. In fact, the J_{H-F} value for the terminal F (368 Hz) is an order of magnitude larger than for the metal-bound F (33 Hz). One of the two values is considerably larger and the other much smaller than $J_{H-F} = 127$ Hz observed[25] for the FHF^-, in which the two F−H bonds are equivalent. The size of $J_{H-F} = 368$ Hz for the terminal F is somewhat comparable with the values of 410−529 Hz reported for HF under different conditions.[26] Since J_{F-F} for free FHF^- is inaccessible, only the calculated values of −133 (MCLR)[27] and 225 Hz (EOM-CCSD)[28] are available for comparison with the $J_{F-F} = 119$ Hz determined for **1**.

(25) Fujiwara, F. Y.; Martin, J. S. *J. Am. Chem. Soc.* **1974**, *96*, 7625. Christe, K. O.; Wilson, W. W. *J. Fluorine Chem.* **1990**, *47*, 117.
(26) McLean, C.; Mackor, E. L. *J. Chem. Phys.* **1961**, *34*, 2207. Mackor, E. L.; Maclean, C.; Hilbers, C. W. *Recl. Trav. Chim. Pays-Bas* **1968**, *87*, 655. Muenter, J. S.; Klemperer, W. *J. Chem. Phys.* **1970**, *52*, 6033. Martin, J. S.; Fujiwara, F. Y. *J. Am. Chem. Soc.* **1974**, *96*, 7632.
(27) Shenderovich, I. G.; Smirnov, S. N.; Denisov, G. S.; Gindin, V. A.; Golubev, N. S.; Dunger, A.; Reibke, R.; Kirpekar, S.; Malkina, O. L.; Limbach, H.-H. *Ber. Bunsen-Ges.* **1998**, *102*, 422. Benedict, H.; Shenderovich, I. G.; Malkina, O. L.; Malkin, V. G.; Denisov, G. S.; Golubev, N. S.; Limbach, H.-H. *J. Am. Chem. Soc.* **2000**, *122*, 1979.
(28) Perera, S. A.; Bartlett, R. J. *J. Am. Chem. Soc.* **2000**, *122*, 1231.

Scheme 1

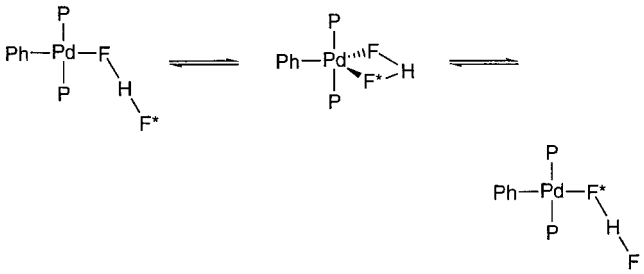

Scheme 2

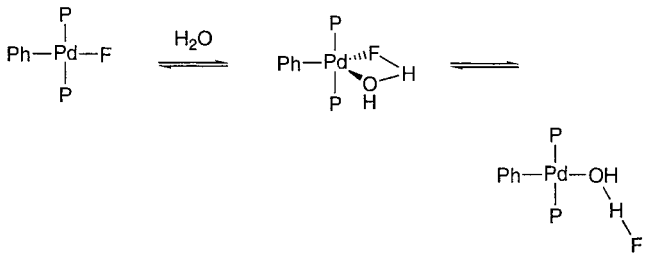

Being of M−F···H−F type, **1** undergoes HF transfer to **2** in solution, resulting in Pd−*F*HF/Pd−*F* interchange (see above).[29] Chemical evidence for HF dissociation from **1** was also obtained. After solutions of **1** in dry CD_2Cl_2 − toluene-d_8 (2:1 v/v) were kept in glass NMR tubes at room temperature for a few days, glass etching was observed and new signals were found in the ^{19}F NMR spectra of the samples, which were assigned to Si−F species. No formation of such species took place when Teflon liners were employed (see above). Furthermore, the products formed upon the thermal decomposition of **1** in anhydrous toluene point to HF dissociation, followed by a series of oxidative addition and reductive elimination reactions, as described earlier.[30]

As demonstrated by the magnetization transfer studies (see above), HF dissociation is a minor contributor to exchange processes occurring in solution of **1** in a low-polar medium. The fastest exchange process between Pd−*F*HF and Pd−FH*F* is concentration independent, suggesting an intramolecular mechanism and ruling out mechanisms that involve elimination of HF or FHF^- from **1**, as well as intermediate formation of associates of two or more molecules of **1**. This intramolecular rearrangement is not influenced by the presence of **2** (see above).

Complexes of the type $[(Ph_3P)_2Pd(Ph)(X)]$ are known to undergo phosphine dissociation in solution (see ref 30 and references therein). However, phosphine dissociation is not involved in the intramolecular rearrangement of **1**, as was established by recording a ^{31}P NMR spectrum (20 °C) of **1** and Ph_3P (1/1) in a 2/1 v/v mixture of CD_2Cl_2 and toluene-d_8. The spectrum exhibited two singlet resonances, at 22.5 ppm from **1** and at −5.5 ppm from free PPh_3, indicative of the lack of fast exchange between the complex and the free phosphine.

In accord with all experimental data, the mechanism for exchange shown in Scheme 1 may be viewed as an intramolecular version of the widely recognized associative mechanism for ligand exchange in square-planar complexes of Pd(II).[31] The negative entropy of activation for the process (-56.1 ± 9.6 J mol^{-1} K^{-1}) is remarkably close to the values measured for a number of unimolecular organic rearrangements proceeding via a cyclic transition state.[32] Examples include the Cope rearrangement of 1,2-divinylcyclobutane (−48.9 J mol^{-1} K^{-1})[33] and the Claisen phenyl allyl ether rearrangement (−50.2 J mol^{-1} K^{-1}).[34] Bent hydrogen bonding required for the η^2-FHF Pd species proposed (Scheme 1) finds a precedent in the X-ray structure of $[Cp^*_2Nb_2F_6(\mu\text{-FHF})_2]$ containing two FHF ligands bridging two niobium centers.[14]

It is not clear to what extent the Pd−F bond in **1** weakens before the terminal fluorine coordinates to Pd, but full ionization to a tight ion pair $\{[(Ph_3P)_2Pd(Ph)]^+[FHF]^-\}$ seems unlikely in media of low polarity and is certainly inconsistent with the negative entropy of activation (-56.1 ± 9.6 J mol^{-1} K^{-1}). Furthermore, the ability of both HF and H_2O to form hydrogen bonds suggests that the intramolecular bifluoride rearrangement in **1** may be closely related to the water-promoted reversible Pd−F bond ionization in **2** and other fluoride complexes of the series $[(Ph_3P)_2Pd(4\text{-}C_6H_4X)(F)]$.[11b] Under identical conditions, the slowest hydrolysis rate had been observed for X = Cl, whereas all other substituents X, *both* stronger electron donors (H, Me, MeO) and stronger electron acceptors (CF_3, NO_2), facilitated Pd−F ionization. This then-unexpected effect could be rationalized only in terms of the double-site coordination of water to the fluoride ligand and the Pd center (Scheme 2).[11b] While an electron-withdrawing X would facilitate nucleophilic attack of water on the metal center, an electron-donating X would favor hydrogen-bonding interactions between the fluoride ligand and H_2O. Because coordination of each of the two types *alone* would result in some correlation between the rate of Pd−F ionization and electronic properties of X, the lack of correlation observed points to an overlap of the two opposite effects. In addition to the negative entropy of activation for the intramolecular F/F exchange in **1**, the above observations along with clear similarity of processes outlined in Schemes 1 and 2 suggest that full Pd−F ionization is unlikely in either case.

Conclusions

A palladium bifluoride complex, $[(Ph_3P)_2Pd(Ph)(FHF)]$ (**1**), has been studied by X-ray diffraction, IR and VT

(29) (a) The negative entropy of activation for this process ($\Delta S^\ddagger = -92.9 \pm 27.6$ J mol^{-1} K^{-1}) is consistent with an associative exchange between the exchange partners[29b] or geometry restrictions for **1** in the transition state for HF dissociation. These restrictions are likely dictated by an increase in strength of destabilizing Pd−F filled/filled repulsions[17] upon HF dissociation, which are alleviated by the geometry-controlled push−pull interactions along the PhPdF axis[15] and/or PdF···HC (PPh_3) contacts.[16] Similarly, negative $\Delta S^\ddagger$ values are exhibited by pyrolytic Ei eliminations (e.g., EtBr to HBr and C_2H_4) due to the syn geometry required for the transition state.[29c] Bimolecular exchange may involve hydrogen bonding of the F ligand in **2** to the bilfuoride hydrogen in **1**: e.g., $[(Ph_3P)_2(Ph)Pd(\mu\text{-}F\cdots H(F)\cdots F)Pd(Ph)(Ph_3P)_2]$. (b) Alder, R. W.; Baker, R.; Brown, J. M. *Mechanism in Organic Chemistry*; Wiley: New York, 1971. (c) March, J. *Advanced Organic Chemistry*, 3rd ed.; Wiley-Interscience: New York, 1985; pp 896−900.

(30) Grushin, V. V. *Organometallics* **2000**, *19*, 1888.

(31) Cotton, F. A.; Wilkinson, G. *Advanced Inorganic Chemistry*, 5th ed.; Wiley-Interscience: New York, 1988.

(32) Gordon, A. J.; Ford, R. A. *The Chemist's Companion: A Handbook of Practical Data, Techniques, and References*; Wiley-Interscience: New York, 1972; p 140.

(33) Kosower, E. *An Introduction to Physical Organic Chemistry*; Wiley-Interscience: New York, 1968.

(34) Rhoads, S. J. In *Molecular Rearrangements*; deMayo, P., Ed.; Wiley-Interscience: New York, 1963; p 655.

^{1}H, ^{19}F, and ^{31}P NMR spectroscopy, and ^{19}F NMR magnetization transfer. The Pd bifluoride is fluxional in solution at room temperature due to F/F interchange. When the latter is frozen at −60 °C, the structure of **1** in solution is similar to the solid-state X-ray structure. Although all structural and spectroscopic data point to MF···HF rather than M···FHF character for **1**, ^{19}F NMR magnetization transfer experiments have demonstrated a minor contribution of HF dissociation to the exchange. The main process that governs F/F exchange in **1** is intramolecular ($\Delta H^{\ddagger} = 33.7 \pm 2.1$ kJ mol^{-1}; $\Delta S^{\ddagger} = -56.1 \pm 9.6$ J mol^{-1} K^{-1}), which is proposed to occur via the pentacoordinate intermediate [$(Ph_3P)_2Pd(Ph)(\eta^2$-FHF)]. DFT calculations for two model Pd bifluoride complexes [$(R_3P)_2Pd(Me)(FHF)$] (R = H, Me) indicate virtually unrestricted rotation around the Pd−FHF bond.

Experimental Section

All samples were prepared in a glovebox (N_2) with deuterated solvents that were carefully dried using standard procedures and stored over freshly calcined molecular sieves (4 Å). Bifluoride **1** and its σ-methyl analogue were synthesized from [$(Ph_3P)_2Pd_2(R)_2(\mu$-OH$)_2$] (R = Ph, Me) with $Et_3N(HF)_3$ (TREAT HF) in the presence of Ph_3P, as described previously.[11] For all NMR experiments, freshly prepared solutions in rigorously dry CD_2Cl_2 and toluene-d_8 (2:1 v/v) were placed in Teflon liners inside standard 5 or 10 mm glass NMR tubes. For heat-transfer purposes, the space between the liner and the glass tube was filled with the pure CD_2Cl_2−toluene-d_8 mixture (2/1 v/v). The samples were sealed and used for NMR studies immediately after preparation. The ^{1}H, ^{31}P, and ^{19}F NMR spectra and decoupled spectra were obtained with a 400 MHz Varian Unity INOVA spectrometer with a 4-nucleus probe.

X-ray Analysis. X-ray-quality crystals of **1** were obtained from dichloromethane−hexanes. Data collection for a 0.23 × 0.24 × 0.40 mm crystal of **1** was carried out with a Bruker SMART 1K CCD system. Selected crystallographic data for **1** are collected in Table 1. The structure was solved using XS (Shelxtl) and refined using Shelxtl software package by full-matrix least squares on F^2 for 855 parameters. All hydrogen atoms except H1 and H71 were idealized as riding hydrogens. Full details of the crystallographic study is presented in the Supporting Information.

Dynamic NMR Studies. Magnetization transfer experiments were performed on a GE NMR Instruments Omega PSG spectrometer operating at 361.31 MHz for ^{1}H and 339.40 MHz for ^{19}F. The high-power ^{19}F 90° observe pulse was 10 μs, while the power for the selective 180° inversion pulse was adjusted on resonance to give a selective pulse width of 5.3 ms. The delay time between the selective inversion pulse and the 90° readout pulse was arrayed from 1 to 400 ms in order to map out the time dependence of the intensity changes (^{19}F T_1's were approximately 20 ms for Pd−*F*HF, 40 ms for Pd−FH*F*, and 60 ms for Pd−*F*).

The general protocol for the magnetization transfer experiments was to selectively invert one site and to monitor the return to equilibrium of the inverted site as well as the transient changes in intensity of the exchange partner(s). The experiment was then repeated by selectively inverting the other site(s). The exchange matrix was formulated in the standard fashion,[35] and rate constants were obtained by iterative adjustment of the equilibrium and initial magnetization integrated intensities, the T_1's, and the rate constant(s) to provide the least-squares best fit to the experimental data along with standard deviations for the parameter estimates.[24]

DFT Calculations. All DFT calculations were performed with UniChem's DGauss program[36] on a Silicon Graphics Origin 2000 computer. The basis sets were the local spin density optimized Gaussian basis sets DZVP.[37] Except where otherwise noted, the geometry of each molecular structure was fully optimized (no constrained metric parameters) at the self-consistent gradient-corrected (nonlocal) energy level with the Becke exchange functional[38] and the Perdew correlation functional.[39] Vibrational frequencies were determined at the same energy level in order to obtain zero-point energies and vibrational thermal corrections for use in computing thermochemistries of reaction.

Acknowledgment. We thank Dr. David L. Thorn for a fruitful discussion.

Supporting Information Available: Full details of the X-ray crystallographic study of **1**. This material is available free of charge via the Internet at http://pubs.acs.org.

OM000637R

(35) (a) Binsch, G. In ref 20, Chapter 3, pp 51−52. (b) Johnson, C. S.; Moreland, C. G. *J. Chem. Educ.* **1973**, *50*, 477.
(36) (a) Andzelm, J.; Wimmer, E. *J. Chem. Phys.* **1992**, *96*, 1280. (b) Andzelm, J. In *Density Functional Theory in Chemistry*; Labanowski, J., Andzelm, J., Eds.; Springer-Verlag: New York, 1991; p 155. (c) UniChem and DGauss are products of Oxford Molecular Group, Oxford, England.
(37) Godbout, N.; Salahub, D. R.; Andzelm, J.; Wimmer, E. *Can. J. Chem.* **1992**, *70*, 560.
(38) Becke, A. D. *Phys. Rev. A* **1988**, *38*, 3098.
(39) Perdew, J. P. *Phys. Rev. B* **1986**, *33*, 8822.